A&A 499, 627–632 (2009)
DOI: 10.1051/0004-6361/200811406

Astronomy & Astrophysics

The digitized archive of the Arcetri spectroheliograms. Preliminary results from the analysis of Ca II K images

I. Ermolli, E. Marchei, M. Centrone, S. Criscuoli, F. Giorgi, and C. Perna

INAF - Osservatorio astronomico di Roma, via Frascati 33, 00040 Monte Porzio Catone, Italy
e-mail: ermolli@oaroma.inaf.it

Received 24 November 2008 / Accepted 6 March 2009

ABSTRACT

Context. The increasing interest in the recovery of historic data and the availability of new hardware resources is leading to projects to digitize photographic archives of astronomical observations. In addition to preservation, solar archives are digitized because the observations stored in such archives have the potential of providing unique information about solar magnetism, which can improve knowledge about long-term solar changes.
Aims. The solar tower of the Arcetri Astrophysical Observatory produced synoptic observations of the solar atmosphere from 1926 to 1974. The photographic archive contains about 13 000 plates of full-disk Ca II K and H_α spectroheliograms acquired during about 5000 observing days. The program for the digitization and distribution of the images of this archive was carried out at the Rome Astronomical Observatory and is now complete.
Methods. Nearly 13 000 plates were scanned with a commercial device and stored on DVD, as well as in a database accessible online. Image processing was developed for the reduction of the data and their photographic calibration.
Results. The obtained digital archive provides the astronomical community with the Arcetri historical solar observations and with measurements of solar features identified in such observations. As an example, we show some preliminary results concerning the temporal variability of facular regions identified in the time-series of Ca II K observations.
Conclusions. Existing programs studying solar activity and variability, as well as new scientific projects, will benefit from the Arcetri digital archive, since it extends the temporal baseline of digital full-disk solar observations, and it provides data for the inter-calibration of results obtained from measurements performed in similar observations.

Key words. Sun: chromosphere – Sun: faculae, plages – Sun: activity – techniques: image processing – astronomical data bases: miscellaneous

1. Introduction

There is an increasing interest in the digitization of observations stored in astronomical plate archives, both for the preservation of their content and for their distribution to researchers. For instance, solar archives store synoptic observations of the full-disk solar atmosphere, which can be employed to study long-term solar variability.

Several projects devoted to the digitization of solar photographic archives began in the last decade. Mt Wilson and Koidakanal Ca II K spectroheliogram time-series have been digitized (Foukal 1996; Ulrich et al. 2004; Lefebvre et al. 2005; Makarov et al. 2004), and other similar series are now being processed as well (Dorotovic et al. 2007). In this framework, we present the digital archive of Ca II K and H_α spectroheliogram observations taken at the Arcetri Astrophysical Observatory from 1926 to 1974. The interest in the digitization of the Arcetri solar photographic archive is that the stored observations are among the oldest such data taken in Europe (for a list of synoptic programs carried out before 1950, see Mouradian & Garcia 2007). Moreover, the Arcetri archive shows the peculiarity of having a large fraction of plates carrying specific information for the photographic calibration of the observation. On the other hand, the temporal coverage of the Arcetri time-series and the number of stored plates are rather small with respect to those of other archives of synoptic solar observations (Ermolli et al. 2007b).

In this paper we describe the content of the Arcetri photographic solar archive (Sect. 2), the digitization work (Sect. 3), and the procedures developed for reduction (Sect. 4) and photographic calibration of the obtained data (Sect. 5). We present some results obtained by analyzing the digital images of the Ca II K time-series (Sect. 6) and briefly mention the next steps of our work (Sect. 7).

2. The Arcetri solar archive

The Arcetri photographic archive contains 12 917 plates of full-disk Ca II K and H_α spectroheliograms, which were acquired during 5042 observing days at the "Donati" solar tower telescope of the Arcetri Astrophysical Observatory (Florence, Italy), from 24 July 1926 to 15 September 1974 (Godoli & Righini 1950). In particular, the archive contains 5976 and 6941 Ca II K and H_α observations, respectively. There is an average of about 100 Ca II K and 120 H_α plates per year during the whole period. The number of plates per year quadruples from 1956 to 1961. At the time of observation, the instrument had a grating of 600 lines/mm and a ruled area of 100 mm × 100 mm, with a dispersion of 0.33 mm/Å at 3934 Å.

Several instrumental changes occurred during the over forty years in which the Arcetri spectroheliograph was utilized. These include the use of additional lenses and changes of the slit

positions, which improved the image definition and monochromaticity, and decreased the stray-light level. For instance, observation log-books showed that on 23 July 1938 the testing of an additional field lens started to improve the image definition. This lens was utilized starting from 20 January 1939. In the same period the utilization of filters at the first slit also started. A Schott UG_2 filter was utilized for the Ca II K observations from 15 October to 30 December 1938, then replaced with a Schott UG_3 filter. A Schott RG_2 filter was utilized for the H_α observations from 15 October to 29 July 1939. Moreover, on 25 May 1953, the position of the 2nd slit was modified, decreasing its distance from the plate from 1.3 cm to 2 mm. We note these instrument changes because they mark a few discontinuities in the data collection. The instrumentation that was used to acquire these observations is no longer available.

The plates stored in the archive have different dimensions and contents. The ones acquired before 1936 measure 9×18 cm and have two images of the Sun with a diameter of 6.5 cm (13% of the whole archive); later plates measure 9×12 cm and have just one image of the Sun with a diameter of about 6.5 cm (87% of the whole archive). 5% of the data is stored on acetate negatives. The size of the solar disk image on most plates corresponds to an image scale of about 0.033 mm/arcsec.

Observatory log-books show that 36 different photographic products from 8 different manufactures were used during the whole period of observations. The spectroheliograms obtained after 22 February 1938 carry calibration exposures obtained through a Zeiss *K* 58 step filter. This step filter was calibrated both photoelectrically and photographically specially for the study presented by Caccin et al. (1970). At first, only one photometric mark was stored on the plates, by placing the Zeiss filter on the first slit and gathering the radiation emitted from the solar-disk center. Starting from September 1947, two photometric marks were stored on the plates by changing the width of the first slit. From August 1948 onwards, three photometric marks were stored on each plate: the first one was obtained with the radiation emitted in the Ca II K or H_α from the solar-disk center, the second one in the radiation of the near-continuum to the line in question, and the third one always in the same continuum, but by doubling the width of the first slit. The log-books also note that the velocity of the drive motors that translate the slit position during the wedge exposure was equal to the one used during the solar image exposure. Whether more observations were obtained during the same day or not, the calibration wedge was stored only on the latest plate exposed. However, since all the plates obtained on the same day were photographically processed at the same time, a single calibration wedge can be used for all the specthroheliograms of the same day.

The Arcetri solar tower and spectroheliograph showed from the very beginning limitations for the study of details of the solar surface (Gasperini et al. 2004; Righini 2003), as the spatial scale of observations were degraded by the local seeing, on average to about 5 arcsec. However, more than 65% of the plates in the archive contain the step-wedge exposures for the calibration of the non-linear response of the photographic emulsion to the flux of the incident radiation. The Arcetri series is thus particularly suitable for the study and comparison of different calibration methods based on either calibration exposures or other criteria, such as the use of solar intensity limb darkening or intensity distributions. Table 1 gives the transmission factors for the step-wedge exposures recorded in the Arcetri log-books. These factors were used for the conversion of the plate blackening into plate exposure, as described in Sect. 4.

Table 1. Transmission values of the Zeiss *K* 58 step filter from the observation log-books of the Arcetri Observatory.

λ = 6000 Å	100%	72%	45%	28%	19%	11%
λ = 4000 Å	100%	68%	42%	29%	20%	14%

3. The digitized archive

A preliminary study for the definition of the characteristics of the digitization work was carried out by simultaneously testing three devices on a sample of plates extracted from the archive and covering 1% of the dataset. These devices were two commercial scanners (Epson Perfection 1200, Epson Expression 1680 pro) and a system equiped with a 1k × 1k CCD camera, developed at the University of Rome "Tor Vergata". The selected plates were extracted from the Ca II K time-series; we chose two plates for each available year, one acquired in winter, the other one in summer. This was meant to take into account potential effects of seasonal variations on image content. Test images of the selected plates, as well as of a linear target, were acquired under different settings of the three devices. After analyzing the obtained images, we decided to perform the digitization work by using the Epson Expression 1680 pro commercial scanner, at 1200 dpi and 16 bit significant data.

The selected setting corresponds to a scale of 0.62″/dot in most of the produced digital images. Due to the limitations of the typical local seeing, which during the best conditions was worse than 2″, with a higher scanner settings (e.g. 1600 or 2400 dpi), no space information content would be added to the acquired image. On the other hand, lower resolution settings (e.g. 600 or 800 dpi), would not allow us to resolve some details which occasionally could be present in the observations. Moreover, even though most analyzed plates seemed to be either under- or over-exposed, we decided to store the digital images as 16 bit grey-scale data. We considered that a reduction of dynamic range in using 8 bits would occasionally result in loss of photometric information from the original observation. In fact, the effects of such a reduction depend on the exposure and potential defects of individual plates, and thus have to be evaluated with care for each image. However, more digital products were obtained with the increase of the information content per pixel from 8 to 16 bit. In particular, with the 1200 dpi setting, the image size increases from 13 to 46 Mb assuming 8 and 16 bit data significance, respectively. The instrument and settings so defined allowed the scanning of plates in groups of four for most of the archive; each scan produced a TIFF format 8435 × 11 153 pixel image (179 Mb each) and took about 5 mn.

The digitization of the whole archive took about one year. All the obtained images were stored on DVDs. The digital images were also assembled in a database, which contains for each observing day all the data available and some additional information, such as step-wedge measurements and characteristic curves for the photographic calibration of the images. The database is presently stored on a dedicated PC at the Rome Observatory and can be accessed through a web interface[1].

4. Image processing

Dedicated software was developed to provide automatic reduction of the digitized images. This reduction includes the correction for the scanner response to a flat-field, the separation of each

[1] http://www.mporzio.astro.it/solare/LastreArcetri.htm

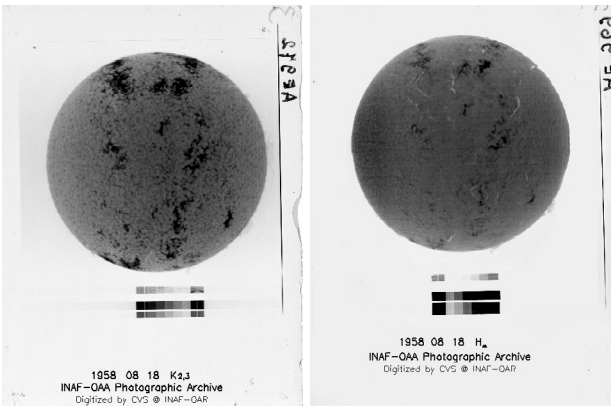

Fig. 1. Example of the digitized images available on-line: Ca II K (*left*) and H_α (*right*) Arcetri spectroheliograms taken on 18 August 1958.

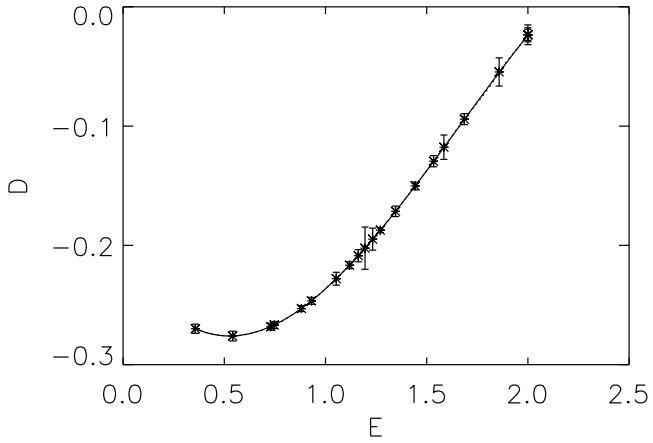

Fig. 2. The calibration curve (solid line) computed for the Ca II K image shown in Fig. 1. Details are given in the text.

solar observation, and the extraction of image pixel values in the step-wedge exposures. This software was developed in the IDL language.

The flat-field response of the scanner was obtained at both the beginning and end (henceforth referred as *B* and *E*, respectively) of each digitization session, by taking an average image of the scanner fluorescent screen. Note that internal scanner calibration scans set the returned data numbers so that points with no obstruction return the maximum pixel value and points with total obstruction return zero pixel value. We found that about 60% of calibration scans contain all the image pixel values at the scanner saturation level of 65 536 digitization units, as expected for a scanner exposed without obstruction. These scans are equally distributed between the *B* and *E* samples. The median of image pixel values for about 70% of *B* scans differs ≈4% from the scanner saturation level. The standard deviation of pixel values in these scans is 6×10^{-3}. On the other hand, the median of image pixel values for about 60% of *E* scans differs less than 0.3% from the scanner saturation level. The standard deviation of pixel values in these scans is 2×10^{-3}. We found that the characteristics of the scanner response were constant during the whole digitization work.

Each image obtained by digitization was divided by the scanner calibration scan acquired closest in time to the processed image. Then, the sub-image corresponding to each solar observation was singled out from each digitized image; couples of images for each individual spectroheliogram, both in FITS (2040 × 2040 pixel) and JPG formats (510 × 680 pixel) were stored (Fig. 1). Whenever the calibration exposures are included in the digitized plate, the image processing also provided from 7 to 21 triplets of average, standard deviation, and median of the transparency values *T* for each step of the calibration wedge. These values were used to evaluate the calibration curve for the photographic calibration of the original observation, as described in the following. Given the number of digitized plates, we first tried to fully automate the step-wedge identification processing. However, the plates are very different from each other: the solar observation and the step-wedge show different shades and positions against the plate background, as well as different dimensions. These differences, together with the presence of plates defects such as lines, large-scale lack of homogeneity, scratches, and over-exposure hampered the running of a completely automated processing. The applied procedure required a post-processing control.

5. Photographic calibration

The photographic calibration constitutes a key step in the processing of the digital images considered in this study. It allows us to relate the image pixel values, which measure the plate blackening at the position corresponding to the image pixel, to the flux of solar radiation incident during the plate exposure.

As presented in the literature (Dainty & Shaw 1974), the most common quantitative measure of photographic output is the optical density *D* of the developed photographic layer. The density is defined as Log_{10} of the opposite of the plate transparency (or transmission) *T*, which, in turn, is given by the relationship between the incident intensity I_i and that transmitted by the plate I_t. The density is usually related to the amount of exposure *E* which was necessary to produce it. The exposure is defined as the product of the intensity *I* of the exposure radiation and the exposure time *t*.

We evaluated the calibration curve, which relates the photographic density (output) to the logarithm of the plate exposure (input), starting from the average value of transparency *T*, and its standard deviation measured at the various steps of the wedge exposure. In particular, following Caccin et al. (1998), we computed the curve through a least squares third-degree polynomial applied to the measured values, after a suitable data rearrangement and interpolation (Fig. 2). The measured values *T* for the various steps of the wedge exposure were sorted in order of increasing exposure. The obtained values, together with intensity values expected by the step-wedge exposure (Table 1), were linearly interpolated in order to produce a 200 × 2 element matrix showing the correspondence between density and intensity for the analyzed image. This matrix was used as input for the polynomial fitting, which was performed by taking into account the standard deviation measurements for the transmission measured in each step. The fitting returned the function coefficients used to obtain the photographic calibration of image pixel values on the digitized image (Fig. 4, left panel).

The evaluation of the calibration curve was performed for each Ca II K image showing a calibration wedge. Figure 3 shows all the obtained curves. Note that the whole sample of Ca II K images can be divided into four sub-samples, depending on both instrument and observation changes occurring during the temporal baseline of the Arcetri observations. However, there is a large scatter among the curves obtained for each sub-sample. The calibration of the Ca II K images stored without step-wedge exposures was performed by using a reference curve. This curve

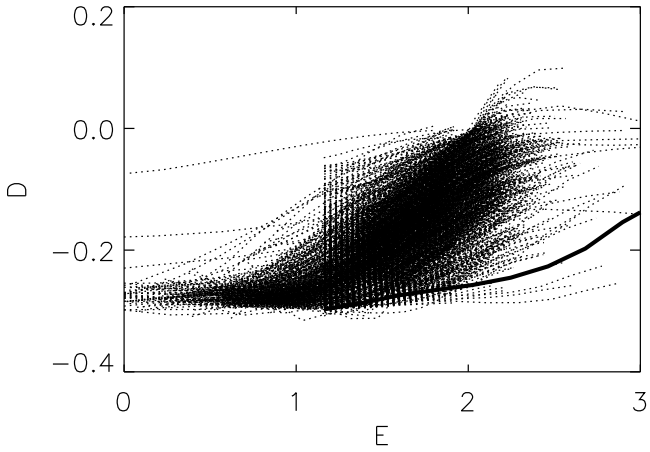

Fig. 3. Calibration curves computed from the whole sample of images with step-wedge exposures obtained by the digitization of the Arcetri Ca II K series. The solid line represents the reference curve used to calibrate the images without step-wedge exposures.

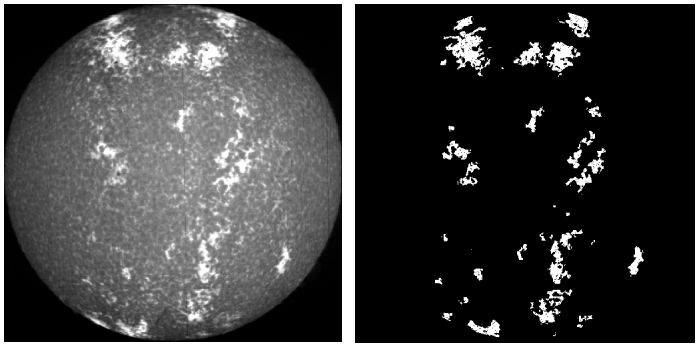

Fig. 4. *Left*: example of images obtained by the reduction and photographic calibration of the produced digital data. *Right*: example of the binary images showing the facular features identified by the processing described in Sect. 6. These images refer to the the Ca II K observation shown in Fig. 1.

was singled out among all the computed ones, since it allows us to calibrate the largest sample of images carrying no specific calibration information by obtaining images in which the intensity pattern on solar observations appears as it is usually seen on modern intensity Ca II K observations of the solar disk. However, the selected curve exhibits a large scatter with respect to most of the computed curves. Some evaluations of uncertainties associated with the use of the reference curve instead of the specific information stored on the original observation are given below.

6. Preliminary results

The project of digitizing the Arcetri archive was mostly driven by the interest in analyzing its time-series of Ca II K observations, to obtain measurements of facular regions over the temporal baseline covered by such an archive. These measurements are used in many fields of solar research. For instance, positional data can be used to study the fine details of the cyclic behavior of solar activity (e.g. Harvey 1992; Ternullo 2007; Solanki et al. 2008). On the other hand, measurements of facular daily position and extent over the solar disk together with evaluations of facular brightness obtained through atmosphere models, can be used to evaluate the time behavior of solar irradiance (e.g. Penza et al. 2003; Walton et al. 2003; Fontenla et al. 2004).

In the following, we describe some preliminary results obtained by performing an automatic determination of the area and position of facular features observed in Arcetri Ca II K data. In particular, we corrected all the images obtained by the processing described above for the intensity center-to-limb variation of the quiet Sun (CLV). For this, we estimated the CLV on each image by computing the quiet Sun intensity values in 20 concentric constant area annuli of the solar disk. Following Brandt & Steinegger (1998), we defined as the quiet Sun 5% of the maximum value of the cumulative intensity histogram in each annulus. The set of computed intensities was used to create the surface representative of the CLV pattern. Each image was divided by the corresponding CLV and subtracted by one. In the following we refer to pixel contrast values on the obtained images. In order to compensate for residual large-scale contrast patterns affecting the analyzed data, each row of the analyzed images was then divided by the quadratic profile which best fits the contrast values of quiet Sun regions along the considered row. Pixels belonging to active regions in each analyzed row were discarded by applying a contrast threshold criterion. The computation was subsequently applied to each column of the analyzed images.

In order to identify the Ca II K features corresponding to facular regions we applied the Ktr decomposition method described by Ermolli et al. (2007a) to contrast images. This method is based on a combination of pixel contrast and connectivity. The method computes a binary mask image for each analyzed observation, in which pixels satisfying the identification criteria were assigned a value of one, with all other pixels set to zero. An example of obtained mask images is given in Fig. 4 (right panel). Note that, because of the link between Ca II K brightness and magnetic flux intensity (e.g. Skumanich et al. 1975; Schrijver et al. 1989) the identified features are assumed also to represent magnetic regions. An automatic determination of the area and position of sunspots observed on Ca II K images was not performed because the analyzed images show the presence of plate emulsion holes and defects, which would strongly limit the accuracy of such measurements.

Facular regions identified on the computed masks were labeled to study the dependence of their position and area with time. In particular, we computed the geometric barycenter of each feature and converted this position into solar coordinates, by taking into account both solar-disk orientation and ephemeris for each observation. The area of features was defined by the number of pixels selected for each identified feature. In order to reduce effects of spurious feature identifications, the analysis was restricted to regions whose geometric barycenter occurs within $r/R_{\rm sun} = 0.97$ on the solar disk.

We visually inspected the time-series of Ca II K images and found that the orientation of the solar observation varies in time. This variation comes from changes affecting both instrumentation and observational procedures during the acquisition of the Arcetri time-series, as well as during the digitization. Therefore, the analysis of the positional data of the identified features is limited by the accuracy of a proper compensation for the image orientation change.

Figure 5 shows the positional results obtained for the subset of analyzed images showing a constant orientation in time. This subset includes all the Ca II K observations taken from January 1945 to December 1963 and spanning two solar cycles. For this subset of images, we determined the number of features whose barycenter occurs within bins of 2 degrees in latitude per month. The obtained butterfly pattern is apparent, with the wings moving from high latitudes equatorward with time. We have not included in this figure any features that have areas ≤50 micro,

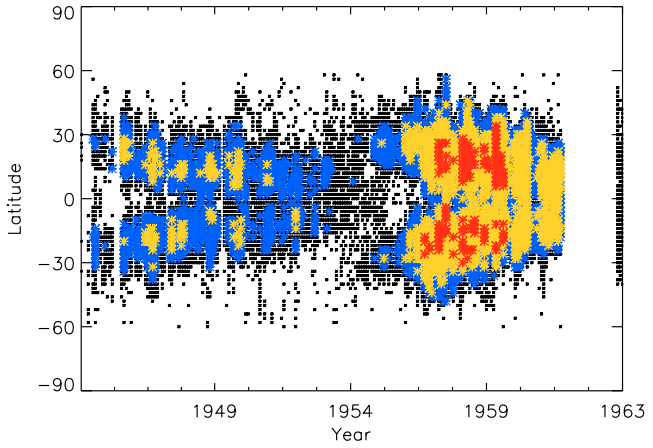

Fig. 5. Butterfly diagram based on the positional data of facular regions identified on digital images of the Arcetri Ca II K spectroheliograms taken from January 1945 to December 1965. Different colors were used to show the number of features identified for each latitude bin. In particular, red, yellow, blue, and black symbols show positional results obtained from more than 100, 30, 10, and from all the identified features, respectively.

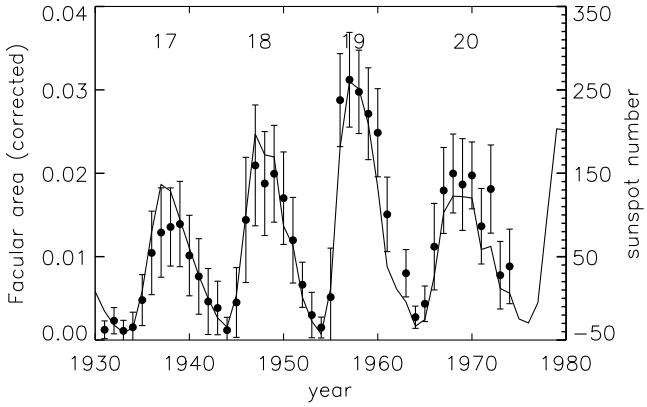

Fig. 6. Temporal variations of the annual median values of the fraction of the solar hemisphere covered by facular regions as measured on the Arcetri images (symbols), together with the annual mean values of the sunspot number (solid line). The area value for each facular region is corrected for foreshortening and expressed as a fraction of the solar hemisphere. The values for the features identified on a given day are summed for each observation. Cycle numbers are marked at the top of each cycle.

when expressed as fraction of the solar hemisphere after the foreshortening correction. However, we find that this pattern is also clearly seen by taking into account all the features identified by our procedure.

We find a general agreement between the latitude values seen in our study early in cycles 18 and 19 and the ones reported by Harvey (1992). However, we note that the latitude values for early features in cycle 19 are higher than the ones obtained for the first appearance of features in cycle 18, in contrast to the results presented by Harvey (1992). Unfortunately we do not have access to the data presented by Harvey (1992), which would allow a quantitative comparison between the two sets of results.

The reliability of the positional measurements presented above depends on the accuracy of the various steps of the image processing, which include the compensation for geometrical distortions of the solar disk, the definition of disk center and radius, and the solar rotational direction. The last step strongly depends on the definition of the image orientation. Any inaccuracies in these steps also affect the reliability of the pattern showing the variation of latitude of the appearance of identified features with time. Since this pattern is thought to be a direct consequence of plasma flows in dynamo models (e.g. Dikpati & Gilman 2009), any processing inaccuracies would lead to an incorrect definition of the mechanisms leading to the emergence of magnetic regions in the solar atmosphere. Therefore, we emphasize once more that the positional measurements presented above are to be considered as preliminary results. We also defer efforts to physically explain such results to future work, after a careful study of orientation on Arcetri images.

Figure 6 shows the temporal variation of the annual median values of the facular area coverage measured on Arcetri images, together with the annual mean value of the sunspot number provided by the NOAA/SDC archive[2]. The area for each identified facular region was corrected for foreshortening and expressed as a fraction of the solar hemisphere. The error bars show the standard deviation of values in each analyzed bin. The temporal variability of the measured facular areas agrees well with the behavior of the international sunspot number series (the computed correlation coefficient is 0.95). However, the compared time-series show some differences in the rank ordering in amplitude of the four solar cycles covered by the analyzed archive, in particular for cycles 17 and 20. These findings, together with the ones concerning the positional data of early features over cycles 18 and 19, suggest that the obtained results might suffer from a variation in time of the observation contents, mainly due to instrumental and observation changes which are seen also in the Arcetri log-books.

In order to evaluate the uncertainties on the obtained measurements due to the reduction applied to the data, we analyzed results obtained applying various processing methods. As an example, we discuss the comparison between the results presented above with those obtained from an analysis of images calibrated with an application of different criteria. In particular, we used a reference curve to calibrate all the data, instead of the curve computed from the specific information stored in the step-wedge exposures available for most of the analyzed images. We find that the median values over annual bins of facular area measurements carried out on images calibrated through a reference curve differ by up to 1% from the values obtained from the images calibrated by using the step-wedge exposures. Note that, although small, these uncertainties would lead to large inaccuracies in the results of models based on these facular measurements, such as the ones inferring irradiance variations.

Assessment of uncertainties on the obtained results associated with instrumental changes occurring during the acquisition of the Arcetri series can be performed only with inter-calibration of the results presented above with those obtained from the analysis of images from different historic archives. This discussion will be addressed in a forthcoming paper (Ermolli et al. 2009).

7. Conclusion

The digitization of the Arcetri solar photographic archive of full-disk spectroheliograms is complete. The obtained images are now available through web access. At present, this database contains reduced-size images (510 × 680 pixels, instead of the 4210×5576 pixel full-size digitized images), for fast display and light on-line storage. Science quality full-size FITS images are

[2] http://www.ngdc.noaa.gov/stp/SOLAR/SSN/ssn.html

available by request, but soon will be freely distributed through the web site.

The electronically-accessible archive of Arcetri observations is the primary result of the work done. Procedures for the reduction and preliminary photographic calibration of the produced images were also developed during the digitization work. The application of these procedures to Ca II K images, together with subsequent processing, based upon modified versions of methods presented in the literature, allowed us to obtain preliminary measurements of the position and area of facular regions over the period covered by the Arcetri archive.

The next step in our work will be the development of procedures for the best photographic calibration and subsequent processing of the produced images, in order to allow accurate and reliable measurements of solar features from the analysis of such data. For instance, the authors are seeking a suitable way of automatic evaluation of image orientation. Consecutive observations marking solar rotation could be used to perform a determination of the orientation of the solar images. Moreover, when enough features are visible, analysis of their distribution over the solar disk could also allow an evaluation of the orientation of the activity belts in each image. Knowledge of the image orientation is required for an extension of the positional analysis of facular regions to the whole period covered by the Arcetri Ca II K observations, as well as for reliable evaluation of patterns of solar rotation based on motions of features identified in these observations. Moreover, the reduction and standard calibration of images from the H_α time-series will be completed in order to provide the community with the digital data produced.

Acknowledgements. Prof. Bruno Caccin suggested the digitization of the Arcetri solar archive and its scientific exploitation. We are grateful to Dr Fabio Cavallini and the Arcetri Solar Group for providing the photographic archive. This project was financed by Regione Lazio in 2003–2005. We thank Prof. Alberto Righini, Prof. Sami K. Solanki, and the Tor Vergata Solar Group for interesting and helpful discussions. The authors acknowledge Prof. Roberto Buonanno for having strongly supported the CVS project.

References

Brandt, P., & Steinegger, M. 1998, Sol. Phys., 177, 287
Caccin, B., Falciani, R., Moschi, G., & Rigutti, M. 1970, Sol. Phys., 13, 33
Caccin, B., Ermolli, I., Fofi, M., & Sambuco, A. M. 1998, Sol. Phys., 177, 295
Dainty, J. C., & Shaw, R. 1974, Image Sci. (New York: Academic Press)
Dikpati, M., & Gilman, P. A. 2009, Space Sci. Rev., in press
Dorotovic, I., Journoud, P., Rybak, J., & Sykora, J. 2007, The Physics of Chromospheric Plasmas, ed. Heinzel, P., Dorotovic, I., & Rutten, R. J., ASP Conf. Ser., 368, 3
Ermolli, I., Criscuoli, S., Centrone, M., Giorgi, F., & Penza, V. 2007a, A&A, 465, 305
Ermolli, I., Tlatov, A., Solanki, S., Krivova, N., & Singh, J. 2007b, The Physics of Chromospheric Plasmas, ed. Heinzel, P., Dorotovic, I., & Rutten R. J., ASP Conf. Ser., 368, 533
Ermolli, I., Solanki, S. K., Tlatov, A. G., et al. 2009, ApJ, in press
Fontenla, J. M., Harder, J., Rottman, G., et al. 2004, ApJ, 605, L85
Foukal, P. 1996, Geophys. Res. Lett., 23, 2169
Gasperini, A., Mazzoni, M., & Righini, A. 2004, Giornale di Astronomia, 3, 23
Godoli, G., & Righini, A. 1950, Mem. SAIt., 21, 4
Harvey, K. 1992, ASP Conf. Ser., 27, 335
Lefebvre, S., Ulrich, R. K., Webster, L. S., et al. 2005, Mem. SAIt., 76, 862
Makarov, V. I., Tlatov, A. G., Singh, J., & Gupta, S. S. 2004, IAU Symp., 223, 125
Mouradian, Z., & Garcia, A. 2007, The Physics of Chromospheric Plasmas, ed. Heinzel, P., Dorotovic, I., & Rutten, R. J., ASP Conf. Ser., 368, 3
Penza, V., Caccin, B., Ermolli, I., Centrone, M., & Gomez, M. T. 2003, ESA-SP, 535, 299
Righini, A. 2003, Mem. SAIt., 74, 556
Schrijver, C. J., Coté, J., Zwaan, C., & Saar, S. H. 1989, ApJ, 337, 964
Skumanich, A., Smythe, C., & Frazier, E. N. 1975, ApJ, 200, 747
Solanki, S. K., Wenzler, Th., & Schmitt, D. 2008, A&A, 483, 623
Ternullo, M. 2007, Sol. Phys., 240, 153
Ulrich, R. K., Webster, L. S., Varadi, F., et al. 2004, AGU Fall Meeting Abstracts, A3
Walton, S. R., Preminger, D. G., & Chapman, G. A. 2003, ApJ, 590, 1088